ARTICLE

Laser Light Scattering Study on Aggregation of Cellulose Diacetate in Acetone

Ding-hai Xie[a], Xu-hua Li[a], Xi-ling Fang[a], Chun-feng Ma[b*]

a. Technology Center, China Tobacco Guangdong Industrial Co., Ltd., Guangzhou 510385, China
b. Faculty of Materials Science and Engineering, South China University of Technology, Guangzhou 510640, China

(Dated: Received on December 10, 2013; Accepted on December 28, 2013)

We have investigated the properties of cellulose diacetate in solution by using laser light scattering. The cellulose diacetate molecules can form micelles and micellar clusters in acetone besides the individual chains. As the concentration increases, the average hydrodynamic radius $\langle R_{\rm h}\rangle$ linearly increases, whereas the ratio of gyration radius to hydrodynamic radius $\langle R_{\rm g}\rangle/\langle R_{\rm h}\rangle$ linearly decreases. It indicates that the micelles associate and form micellar clusters due to the intermolecular interactions.

Key words: Cellulose diacetate, Laser light scattering, Multi-aggregation form structure

I. INTRODUCTION

Cellulose acetate derived from the natural polymer cellulose has attracted increasing attention since it is an environmentally friendly material [1−3]. Due to the excellent chemical resistance, heat resistance, and burning resistance, it has found wide applications in fabrics, membranes and filaments [4−6].

Generally, cellulose acetate is a semi-synthetic polymer obtained through a two-step reaction involving the esterification of cellulose with acetic acid and the partial hydrolysis of the resultant ester groups. We can obtain cellulose diacetate and cellulose triacetate with acetylation of ca. 55% and 61% in respect to the esterification degree. Such cellulose diacetate can be processed into fibers which are used in many fields such as manufacture of filter tow [7].

Compared with cellulose nitrate and ethyl cellulose, there are less solvents which can dissolve diacetate, and the solution is often under harsh conditions [8]. Acetone has been used as solvent for cellulose diacetate in industries for years. No doubt, the structure of cellulose diacetate in the solution has great influence on its properties. It is critical for controlling the quality of the fiber. However, the dissolution at molecular level is still unclear [9−11]. It is reported that some hydrogen-bonded parts of cellulose diacetate in acetone are still present forming the core of non-soluble domains. This is probably because the crystalline domains of trisubstituted cellulose may hinder the acetylation, and the domains are not soluble in acetone forming aggregates [12].

In the present work, the properties of cellulose diacetate in acetone have been investigated by laser light scattering to understand the structures of cellulose diacetate chains in acetone.

II. EXPERIMENTS

A. Matrials

Cellulose diacetate flake was provided by Nantong Cellulose Fibers Co., Ltd. (Jiangsu, China). The solutions of cellulose diacetate were prepared by dissolving the cellulose diacetate flake in acetone. The concentration of the stock solution was 5.0 mg/mL. The solution was diluted in different concentrations (1−4 mg/mL) for measurements.

B. Laser light scattering

laser light scattering (LLS) measurements of the samples were conducted at 25 °C on an ALV/DLS/SLS-5022F spectrometer with a multi-τ digital time correlator (ALV5000) and a cylindrical 22 mW UNIPHASE He-Ne laser (λ_0=632.8 nm) as the light source In static LLS [13−15], we can obtain the weight-average molar mass ($M_{\rm w}$) and the z-average root-mean-square radius of gyration ($\langle R_{\rm g}^2\rangle^{1/2}$ or written as $\langle R_{\rm g}\rangle$) of scattering objects in a dilute solution or dispersion from the angular dependence of the excess scattering intensity, known as Rayleigh ration ratio $R_{vv}(q)$:

$$\frac{KC}{R_{vv}(q)} \approx \frac{1}{M_{\rm w}}\left(1+\frac{1}{3}\left\langle {R_{\rm g}}^2\right\rangle q^2\right)+2A_2C \quad (1)$$

$$K = \frac{4\pi n^2}{N_{\rm A}\lambda_0^4}\left(\frac{{\rm d}n}{{\rm d}C}\right)^2 \quad (2)$$

*Author to whom correspondence should be addressed. E-mail: msmcf@scut.edu.cn

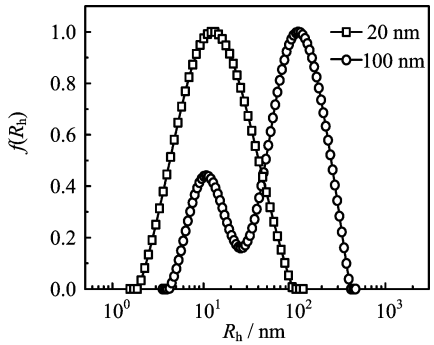

FIG. 1 Typical hydrodynamic radius distribution $f(R_h)$ of cellulose diacetate filtered by different pore-size filters.

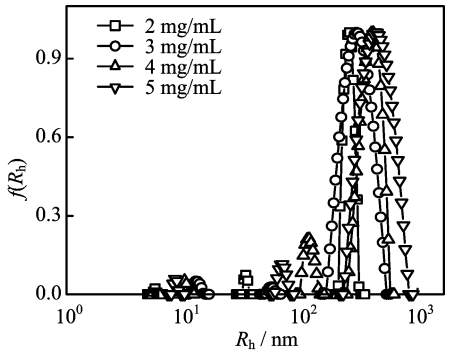

FIG. 2 Typical hydrodynamic radius distribution $f(R_h)$ of cellulose diacetate at different concentrations.

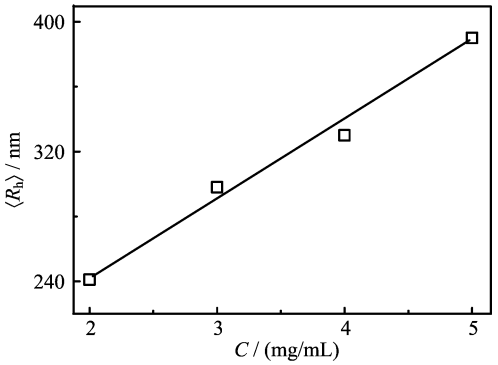

FIG. 3 Concentration C dependence of the average hydrodynamic radius $\langle R_h \rangle$ of cellulose diacetate.

$$q = \frac{4\pi n}{\lambda_0} \sin\left(\frac{\theta}{2}\right) \tag{3}$$

here N_A, dn/dC, n, and λ_0 are the Avogadro number, the specific refractive index increment, the solvent refractive index, and the wavelength of the light in a vacuum, respectively, and A_2 is the second virial coefficient.

In dynamic LLS [16, 17], the intensity-intensity time correlation function $G^{(2)}(q,t)$ was measured to determine the line-width distribution $G(\Gamma)$. For diffusive relaxation, Γ is related to the translational diffusion coefficient (D) of the scattering object (polymer chain or colloid particle) in dilute solution or dispersion by

$$D = \left(\frac{\langle\Gamma\rangle}{q^2}\right)_{C\to 0, q\to 0} \tag{4}$$

and further to hydrodynamic radius (R_h) from the Stokes-Einstein equation:

$$R_h = \frac{k_B T}{6\pi\eta D} \tag{5}$$

where η, k_B, and T are the solvent viscosity, the Boltzmann constant, and the absolute temperature, respectively. Hydrodynamic radius distribution $f(R_h)$ was calculated from the Laplace inversion of a corresponding measured $G^{(2)}(q,t)$ using the CONTIN program. Dynamic LLS measurements were conducted at a small scattering angle θ of 15°. All the solutions were ultracentrifuged to remove impurities before being clarified by Millipore filters. The LLS data points were obtained after the measured values were stable. The value of specific refractive index increment (dn/dC) for cellulose diacetate was 0.11 mL/g at 25 °C [18].

III. RESULTS AND DISCUSSION

Figure 1 shows cellulose diacetate has a unimodal distribution filtered by a 20-nm pore-size filter. Cellulose from wood pulp has typical chain lengths between 300 and 1700 units [19]. Considering that the cellulose diacetate cannot be fully stretched in acetone, the distribution peak located at ∼10 nm can be attributed to the individual cellulose diacetate chains. Once filtered by a 100-nm pore-size filter, cellulose diacetate chains in acetone have a bimodal distribution, indicating that cellulose diacetate chains form aggregates with non-soluble crystalline domains of trisubstituted cellulose as the core and the soluble moieties as the shield [12].

Figure 2 shows the typical hydrodynamic radius distribution $f(R_h)$ of cellulose diacetate at different concentrations filtered by 1-μm pore-size filter. It was reported that cellulose diacetate aggregates can assemble into a network of reversible associates as concentration increases [12]. Thus, the aggregates with a trimodal distribution are attributed to the assembly of cellulose diacetate aggregates. As the concentration increases, the aggregates will overlap, whereas the soluble moieties outside of the aggregate penetrate the core of the other aggregate to form aggregate clusters. Such association is mainly driven by the hydrogen-bonding formed by the OH groups on the backbone of cellulose diacetate. Clearly, the size of the aggregates increases with the concentrations.

Figure 3 shows $\langle R_h \rangle$ of the aggregates increases with

DOI:10.1063/1674-0068/27/03/256-258

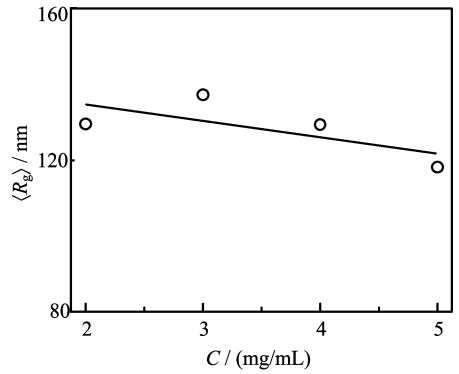

FIG. 4 Concentration C dependence of the average radius of gyration $\langle R_g \rangle$ of cellulose diacetate.

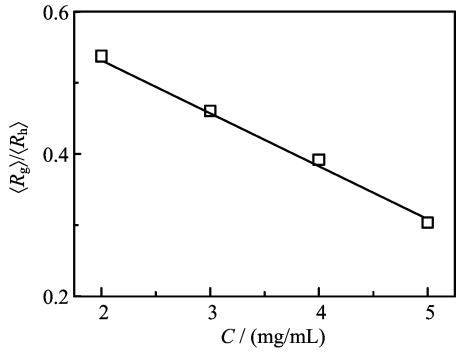

FIG. 5 Concentration C dependence of $\langle R_g \rangle / \langle R_h \rangle$ of cellulose diacetate.

the concentration of cellulose diacetate. The linear dependence indicates the occurrence of reversible association to form aggregate clusters as concentration increases. Figure 4 shows $\langle R_g \rangle$ of the aggregates slightly varies as the concentration of cellulose diacetate increases, indicating that the aggregate cluster has a higher segment density.

Figure 5 shows concentration dependence of $\langle R_g \rangle / \langle R_h \rangle$ of cellulose diacetate. The ratio can reflect the shape and topology of a polymer chain or a particle. For uniform non-draining sphere, hyperbranched cluster, and random coil, $\langle R_g \rangle / \langle R_h \rangle$ are $\sim$0.774, 1.0−1.2, and 1.5−1.8, respectively [20, 21]. A microgel generally has a $\langle R_g \rangle / \langle R_h \rangle$ of 0.6. Clearly, the aggregates have a microgel-like structure at a low concentration reflecting in $\langle R_g \rangle / \langle R_h \rangle \approx 0.6$. As concentration increases, $\langle R_g \rangle / \langle R_h \rangle$ decreases, suggesting that the aggregates tend to form micellar clusters with a denser core due to the intermolecular hydrogen-bonding via OH groups on the backbone of cellulose diacetate.

IV. CONCLUSION

By using laser light scattering, we have investigated the aggregation of cellulose diacetate chains in acetone. In conclusion, the cellulose diacetate chains can form micelles and micellar clusters. As the concentration of cellulose diacetate increases, the average hydrodynamic radius $\langle R_h \rangle$ of cellulose diacetate aggregates linearly increases while the ratio $\langle R_g \rangle / \langle R_h \rangle$ linearly decreases, indicating that the micelles reversibly associate to form micellar clusters due to the intermolecular interactions.

V. ACKNOWLEDGMENTS

This work was supported by China Tobacco Guangdong Industrial Co., Ltd., National Natural Science Foundation of China (No21234003 and No.51303059), and the Fundamental Research Funds for Central Universities.

[1] P. Rustemeyer, Macromol. Symp. **208**, 1 (2004).
[2] J. Ganster and H. P. Fink, *Cellulose and Cellulose Acetate, in Bio-Based Plastics: Materials and Applications*, S. Kabasci, Ed., New York: John Wiley& Sons Ltd. (2013).
[3] S. Fischer, K. Thümmler, B. Volkert, K. Hettrich, I. Schmidt, and K. Fischer, Macromol. Symp. **262**, 89 (2008).
[4] W. M. Raslan, A. T. El-Aref, and A. Bendak, J. Appl. Polym. Sci. **112**, 3192 (2009).
[5] M. Sivakumar, A. K. Mohanasundaram, D. Mohan, K. Balu, and R. Rangarajan, J. Appl. Polym. Sci. **67**, 1939 (1998).
[6] T. Matamá, R. Araújo, G. M. Gübitz, M. Casal, and A. Cavaco-Paulo, Biotechnol. Progress **26**, 636 (2009).
[7] P. Rustemeyer, Macromol. Symp. **208**, 267 (2004).
[8] K. Kamide, T. Terakawa, and Y. Miyazaki, Polym. J. **11**, 285 (1979).
[9] R. S. Stein and P. J Doty, J. Am. Chem. Soc. **68**, 159 (1946).
[10] N. Ahmad, S. Noor, and M. Kaleem, J. Chem. Soc. Pak. **3**, 159 (1981).
[11] H. Kawanishi, Y. Tsunashima, and F. Horii, Macromolecules **33**, 2092 (2000).
[12] L. Schulz, B. Seger, and W. Burchard, Macromol. Chem. Phys. **201**, 2008 (2000).
[13] B. H. Zimm, J. Chem. Phys. **16**, 1099 (1948).
[14] B. Chu, *Laser Light Scattering*, 2nd Edn., New York: Academic Press, (1991).
[15] L. Shen and G. Z. Zhang, Chin. J. Polym. Sci. **27**, 561 (2009).
[16] B. Beme and R. Pecora, *Dynamic Light Scattering*, New York: Plenum Press, (1976).
[17] J. F. Li, Y. J. Lu, G. Z. Zhang, and C. Wu, Chin. J. Polym. Sci. **26**, 775 (2008).
[18] B. Pintarić, M. Rogošić, and H. J. Mencer, J. Mol. Liq. **85**, 331 (2000).
[19] D. Klemm, B. Heublein, H. P. Fink, and A. Bohn, Angew. Chem. Int. Ed. **44**, 3358 (2005).
[20] W. Burchard, *Light Scattering Principles and Development*, W. Brown, Ed., Oxford: Clarendon Press, 439 (1996).
[21] J. F. Douglas, J. Roovers, and K. F. Freed, Macromolecules **23**, 4168 (1990).

DOI:10.1063/1674-0068/27/03/256-258